Osmoregulatory performance and immunolocalization of Na+/K+-ATPase in the branchiopod Artemia salina from the Sebkha of Sidi El Hani (Tunisia)

Imene Sellami, Guy Charmantier, Hachem B. Naceur, Adnane Kacem, Catherine Lorin-Nebel

Osmoregulatory performance and immunolocalization of Na^+/K^+-ATPase in the branchiopod *Artemia salina* from the Sebkha of Sidi El Hani (Tunisia)

Imene SELLAMI [1,2], Guy CHARMANTIER [1], Hachem B. NACEUR [2], Adnane KACEM [2], Catherine LORIN-NEBEL [1*]

[1] Univ. Montpellier, UMR MARBEC (CNRS, IFREMER, IRD, UM), France

[2] LR14ES06 Bioressources, Integrative Biology and Valorization, Higher Institute of Biotechnology of Monastir, University of Monastir, Avenue Tahar Hadded, BP 74, 5000 Monastir, Tunisia

* Corresponding author : Catherine Lorin-Nebel, catherine.lorin@umontpellier.fr

Abstract

Artemia salina is an extremophile species that tolerates a wide range of salinity, especially hypertonic media considered lethal for the majority of other aquatic species. In this study, *A. salina* cysts were hatched in the laboratory and nauplii were acclimated at three different salinities (60, 139 and 212 ppt). Once in the adult phase, their hemolymph osmolality was measured. The animals were strong hypo-osmoregulators in the entire range of tested salinities, with up to 10 fold lower hemolymph osmolalities than their surrounding environment. Immunostaining of Na^+/K^+-ATPase was done on sections and on whole body mounts of adults in order to localize the ionocytes in different organs. An intense Na^+/K^+-ATPase immunostaining throughout the cells was observed in the epithelium of the ten pairs of metepipodites. A positive immunoreactivity for Na^+/K^+-ATPase was also detected in the maxillary glands, in the epithelium of the efferent tubule and of the excretory canal, as well as in the anterior digestive tract. This study confirms the strong hypo-osmotic capacity of this species and affords an overview of the different organs involved in osmoregulation in *A. salina* adults.

Keywords: *Artemia salina,* hypo-osmoregulation, Na^+/K^+-ATPase, immunolocalization, metepipodites, maxillary glands

1. Introduction

Artemia salina (Linnaeus, 1758) is part of a complex of euryhaline species of branchiopod crustaceans qualified as an animal extremophile with an exceptionally wide salinity tolerance among animals, and particularly an ability to survive and thrive in hypertonic media, a "forbidden environment" from which most metazoans are excluded as stated by Eads (2004) (Abatzopoulos et al., 2002; Browne and Bowen, 1991; Clegg and Trotman, 2002). These animals have attracted the attention of scientists over decades and have been the subject of extensive studies in order to understand the mechanisms allowing them to tolerate ionic and osmotic stresses imposed by their environment.

These remarkable crustaceans are able to withstand ionic contents and salinities that, in their upper values, are lethal for the majority of other aquatic species, ranging from 9 ppt (Brisset et al., 1982) to 340 ppt (Gajardo and Beardmore, 2012; Post and Youssef, 1977) and up to crystallizing brine close to 600 ppt (Croghan, 1958a, b). *Artemia salina* is a highly potent hypo-osmotic regulator in media more concentrated than one third of seawater (salinity of about 11 ppt corresponding to an osmolality of 300 $mOsm.kg^{-1}$). For instance, early studies had shown that its hemolymph osmolality is maintained between 400 and 800 $mOsm.kg^{-1}$ for salinities ranging from 34 to 340 ppt (1000 to 10 000 $mOsm.kg^{-1}$) (Croghan, 1958b).

Such levels of hypo-osmoregulation suppose the existence of powerful ion excretion abilities in order to compensate the passive invasion of ions from the concentrated external medium. Moreover, animals have to limit water loss by osmosis, but water uptake mechanisms are not well known in crustacean, notably in those high-salinity environments. In larvae, Conte (1984) has extensively described the mechanisms of osmoregulation in the nauplii of *A. salina* that use a special salt-secreting gland, also called salt gland or neck or nuchal organ, to excrete salts that penetrate by diffusion. Similarly, Russler and Mangos (1978) have shown that this organ is the main route for sodium excretion.

In adult *A. salina*, different studies have shown a similarity between their mechanisms of osmoregulation and those proposed for marine teleosts and hypo-regulating crustaceans (Croghan, 1958b, c, d; Copeland, 1967; Smith, 1969a, b). Brine shrimps have well-developed active mechanisms for absorbing NaCl from the gut lumen to the hemolymph. Hence, water follows passively to compensate water lost by osmosis to the external concentrated medium (Croghan, 1958d). Also in adults, sodium and chloride, which enter the body through diffusion given their high concentration in the external medium, are excreted to the medium by specialized organs acting as gills, the metepipodites. The ten pairs of flattened, leaf-like

metepipodites borne by the phyllopods have been described as the sites of active outward transport of ions (Copeland, 1967; Croghan, 1958c).

In particular, a detailed study of the metepipodites of *A. salina* was conducted by Copeland (1967). Using silver nitrate, he confirmed that the metepipodites were the site of ion (chloride) exchanges, a finding reported earlier by Croghan (1958c) and later confirmed by other authors (Holliday et al., 1990). Copeland's ultrastructural exploration revealed the presence and association of two types of cells in the metepipodites, the "light" and "dark cells". The latter are columnar cells with projected stellate flanges; they extend from the apical cuticle to the basal membrane lining the hemolymph, i.e. they face the external medium as well as the hemolymph, and they present deep interdigitations with the light cells. Stacks of mitochondria, called "mitochondrial pumps" by Copeland, are located in the dark cells in close association with their membrane, particularly in their projections. From these observations, Copeland concluded that the metepipodites represent "a highly specialized tissue for the secretion of salt". Given the location of the dark cells, their ultrastructural features and particularly the abundance of mitochondria in their cytoplasm, "it would appear likely that the dark cell is responsible" for the "release of salt to the external environment" (Copeland, 1967). This hypothesis was confirmed by later experimental findings. In fact, the crude homogenates of metepipodites showed a very high specific enzyme activity of Na^+/K^+-ATPase, which increased proportionally with the salinity of the external medium (Holliday et al., 1990). The same author found that the digestive tract and maxillary glands also had a high Na^+/K^+-ATPase content, which suggests that these organs are also involved in ion transports and probably for a part in osmoregulatory processes. Membrane-bound Na^+/K^+-ATPase was partially purified from *A. salina* nauplii (Morohashi and Kawamura, 1984) and the α isoform of the enzyme was isolated in salt glands and intestine of nauplii (Cortas et al., 1989). Also in naupliar larvae, Na^+/K^+-ATPase α and β isoforms were immunolocalized in the basal membranes of the salt gland cells (Sun et al., 1991) and the mRNA expression of their $\alpha 1$ and $\alpha 2$ isoforms was quantified in the same organs (Conte, 2008; Escalante et al., 1995; Sun et al., 1992). While the localization of the enzyme is known in the larval salt gland, to our knowledge surprisingly few reports are available regarding the localization of Na^+/K^+-ATPase in adult *Artemia*. Recently, an illustration of the presence of Na^+/K^+-ATPase in a metepipodite of *A. franciscana* has been made available in a preliminary report (Drenth, 2017).

The present study aims to confirm the ability of *A. salina* to osmoregulate at very high salinities, and to determine the localization of Na^+/K^+-ATPase in the metepipodites, maxillary glands and digestive tract of adults, in order to improve the understanding of osmoregulatory mechanisms allowing a Tunisian *Artemia salina* population (from the hyper-saline lagoon Sebkha of Sidi El Hani) to withstand high salinities.

2. Materials and methods

2.1. Cysts sampling

Artemia cysts were collected in spring 2017 from the banks of the hypersaline Sebkha of Sidi El Hani where the salinity exceeded 280 ppt.

The Sebkha of Sidi El Hani is a NW–SE lengthened depression in the Sahel area (eastern Tunisia) (Fig. 1). The Sidi El Hani discharge area is approximately 370 km^2 and its average water depth is 0.4 m, and 0.8 m at some locations (Fig. 1). The seasonal temperature fluctuates between 2 and 13 °C in winter and between 33 and 39 °C in summer (Ali et al., 2013). The seasonal average of salinity oscillates between a minimum of 180 ppt in winter registered after rainfall and up to 320 ppt in summer. The ionic composition of Sidi El Hani is mostly based on Na^+ (115 gL^{-1}), Cl^- (191 gL^{-1}), Mg^{2+} (8 gL^{-1}) and SO_4^{2-} (13 gL^{-1}). The presence of *Artemia* in the site was first reported by (Gauthier, 1928) .

2.2. Culture experiments

Upon collection, cysts were mixed with salt collected in the Sidi El Hani area, for conservation. Once in the laboratory, cysts of *Artemia salina* were cleaned, separated and stored according to the protocol of Sorgeloos *et al.* (1986). Cysts were incubated over 48 hrs in 1 liter of filtered seawater at a salinity of 35 ppt and a temperature of 25 °C, under constant illumination (2000 lux) and continuous aeration to keep them in suspension (Lavens and Sorgeloos, 1996). Following hatching, the nauplii were transferred to 3 containers of 5L filled with water at different salinities, 60, 139 and 212 ppt. These media had been prepared from a mixture of seawater sterilized in an autoclave and raw salt (harvested at the Sebkha of Sidi El Hani). In each container, the salinity of the water was checked using a salinometer (Lovibond SensoDirect con110), and the osmolality was measured with an Advanced Instruments 3300 micro-osmometer in later experiments. The containers were placed at a temperature of 25-27

°C and a photoperiod of 16 hrs L / 8 hrs D. *Artemia* nauplii density was adjusted to about 50 individuals per L. These larvae were fed twice a week by adding 100 ml of Chlorophycea *Dunaliella salina* culture at an approximate density of 100,000 cells.ml^{-1} (the salinity of the microalga culture was the same as that used for the culture of nauplii). Water was renewed once a week to ensure the elimination of *Artemia salina* waste and agglomerated microalgae. Once the adult phase was reached, some animals were fixated for histology, others were transported over 24 hrs in sealed containers to the Marbec laboratory (Montpellier, France) for further experiments.

2.3. Measure of hemolymph osmolality

Hemolymph osmolality was measured in 8-12 adult *A. salina* per condition. According to previous results on different crustacean species (Charmantier, 1998), the animals were exposed directly to the experimental media for 48 hrs in covered beakers filled with water at three different salinities maintained at 24 °C, aerated and covered with parafilm to prevent evaporation. The salinities of the media, 60, 139 and 212 ppt, corresponded to osmolalities of 1737, 4064 and 6192 mOsm.kg^{-1}, according to measures made on an Advanced Instrument Model 3300 micro-osmometer. Prior to sampling, the specimens were carefully rinsed with deionized water, dried on filter paper and quickly immersed into mineral oil to prevent evaporation and desiccation. Remaining adherent water was removed using a hand-made glass micropipette. A second micropipette was then inserted dorsally into the heart to obtain hemolymph samples, which were then immediately measured with reference to a 300 mOsm.kg^{-1} standard solution on a Kalber-Clifton nano-osmometer (Clifton Technical Physics, Hartford, NY, USA) requiring about 30 nl.

2.4. Histology and immunolocalization of Na^+/K^+-ATPase

In order to localize the ionocytes, and to visualize and semi-quantify Na^+/K^+-ATPase, we performed histology, immunofluorescence staining, whole-mounts and microscopic observations. About twenty adult brine shrimp from each salinity condition were fixed for 24 hrs by immersion in Bouin's fixative. Once rinsed in several baths of 70 % ethanol, samples were dehydrated in a graded ethanol series and finally embedded in Paraplast (Sigma). Longitudinal and transverse sections of 4 µm were cut on a Leitz Wetzlar microtome, collected on poly-L-lysine coated glass slides and stored at 37 °C for 48 hrs. One series of

slides was stained using the Masson's Trichrome staining protocol and observed under a Leica Diaplan microscope. The other series was used for *in situ* immunolocalization of Na^+/K^+-ATPase. Slides were dewaxed (butanol and LMR), hydrated through a descending series of ethanol baths (from 100 % to 50 %) and rinsed in phosphate-buffered saline (PBS; 137 mM NaCl, 2.7 mM KCl, 10 mM phosphate buffer, pH 7.4, Sigma). The slides were then immersed for 10 min into 0.02 % Tween 20, 150 mM NaCl dissolved in PBS, pH 7.3. After blocking in 5 % skimmed milk (SM) in PBS at 37 °C for 20 min, the slides were rinsed twice with PBS. Primary labelling was carried out overnight at 4 °C in a wet chamber with the primary monoclonal antibody (α5) mouse anti-Na^+/K^+-ATPase (Hybridoma Bank, University of Iowa) diluted in 0.5% SM-PBS at 10 $\mu g.mL^{-1}$. Using a procedure similar to that of this study, this antibody was shown to specifically react with Na^+/K^+-ATPase in several crustacean species, such as *Porcellio scaber* (Ziegler, 1997), *Homarus gammarus* (Lignot et al., 1999), *Astacus leptodactylus* (Lignot et al., 2004), *Carcinus maenas* (Cieluch et al., 2004), *Crangon crangon* (Cieluch et al., 2005), *Eriocheir sinensis* (Cieluch et al., 2007), *Macrobrachium amazonicum* (Boudour-Boucheker et al., 2014) and *Eurytemora affinis* (Gerber et al., 2016). Once rinsed three times in PBS to remove unbound primary antibody, the sections were incubated for 1 hr with a secondary antibody (donkey anti-mouse Alexa Fluor® 488 (Invitrogen, Life Technologies) at 10 $\mu g \cdot mL^{-1}$ in SM-PBS) and rinsed again three times in PBS. Nuclei of some slides were counterstained using DAPI at 1µg/ml for 6 min, followed by three washes in PBS.

Several protocols of preparation and immunostaining of whole mounts of *A. salina* have been tried. A limitation of antibody penetration was encountered probably due to the cuticle barrier. EDTA, ultrasonic treatment from 5 s to 2 min, and Triton X-100 were tested in different combinations. Positive staining was obtained using ultrasonic pulses at 35 KHz from 10 s to 20 s as indicated thereafter. Even in the best preparations, only some metepipodites of the animals showed positive staining. Following pretreatment with ultrasonic pulses (from 10 s to 20 s) to enhance probe accessibility, whole mounts of *A. salina* adults were pre-incubated in 5 % skimmed milk (SM) in PBS and 0.3 % Triton X-100 (PBS-TX) for 2 hrs at room temperature. After blocking, the animals were rinsed several times with PBS. Primary labelling was carried out overnight at 4 °C in a wet chamber with the primary monoclonal antibody (α5) mouse anti-Na^+/K^+-ATPase (Hybridoma Bank, University of Iowa) diluted at 10 $\mu g.mL^{-1}$ in 0.5 % SM-PBS. Following three rinses in PBS, the specimens were incubated for 3 hrs with a secondary antibody (donkey anti-mouse Alexa Fluor® 488 (Invitrogen, Life

208 Technologies) at 10 µg.mL^{-1}) and rinsed again in PBS. Nuclei of some mounts were
209 counterstained using DAPI at 1 µg.mL^{-1} for 6 min, followed by three washes in PBS.
210 Sections and whole mount preparations were then mounted in an anti-bleaching
211 mounting medium (Immunohistomount, Santa Cruz Biotechnology) and observed with a
212 Leica Diaplan microscope equipped with a special filter for fluorescence (450-490 nm) and
213 coupled to a Leica DC300F digital camera and FW4000 software. Observations and
214 photography of selected slides were conducted using a Leica TCS SP2 confocal microscope
215 of the MRI platform, Montpellier University.
216
217 *2.5. Quantification of the Na^+/K^+-ATPase (NKA) immunostaining intensity in*
218 *phyllopods*
219
220 To determine the relative importance of different phyllopods in ion transport in each
221 salinity condition, we compared the relative fluorescence intensity of immunostaining in
222 metepipodites of *Artemia* adults. Several photographs were taken in 5 individuals for each
223 studied salinity using a constant exposure time. Longitudinal sections were used to visualize
224 the different metepipodites and their Na^+/K^+-ATPase content within an animal.
225 The photographs were analyzed using the public domain ImageJ software (version 1.49, v),
226 according to a protocol successfully used in other crustaceans (Boudour-Boucheker et al.,
227 2013; Gerber et al., 2016; Issartel et al., 2010) and in fish (Ouattara et al., 2009; Riou et al.,
228 2012; Sucré et al., 2012). The intensity of immunostaining, i.e. the staining intensity of the
229 immunolabelled area, was measured by quantifying the pixel intensity of the immunolabeled
230 area using ImageJ software. These measurements were performed using the ImageJ software's
231 "Average Gray Value" parameter, which determines the sum of the gray values of all pixels in
232 the selected area relative to the number of pixels, expressed in calibrated units (optical
233 density). In a second step, the ImageJ software was used to quantify the difference in average
234 pixel intensity of fluorescence between different salinities among metepipodites within the
235 same adults.
236
237 *2.6. Statistics*
238 Statistical analyses (hemolymphe osmolality and fluorescence intensity) were performed
239 using Graphpad Prism (version 6, GraphPad Software Incorporated, La Jolla, CA 268, USA).
240 Normality and homogeneity of variance were respectively checked using D'Agostino-Pearson
241 test and Barlett's test. For data fitting homogeneity of variance requirement, a one-way

ANOVA regarding or regardless salinity as the main factor was performed; critical differences between groups were appraised using the Tukey's multiple comparisons test. For data not fitting homogeneity of variance and data due to the small sample size, a non-parametric KrusKal-Wallis test followed by a multiple comparisons Dunn's test was used. Data are presented as means ± SD, and the level of statistical significance was set at $p < 0.05$.

3. Results

The main results of this study are summarized in Fig. 1S.

3.1. Hemolymph osmolality

Artemia adults were extremely strong hypo-osmoregulators. Their hemolymph osmolality, which ranged between 406±21 and 608 ±16 mOsm.Kg^{-1} in our experiment, was significantly different according to salinity (Fig. 2; one-way ANOVA, $p<0.001$). It is worth noting that hemolymph osmolalities differed by only 202 mOsm.Kg^{-1} between the lower and higher tested salinities that themselves differed by more than 4450 mOsm.Kg^{-1}.

3.2. Morphological description

The morphology of *Artemia* adults is illustrated in Fig. 3. Eleven pairs of phyllopods (Ph1-11) were observed. The ten pairs of flattened leaf-like metepipodites are attached at the middle part of the ten phyllopods, (Me1-10). The eleventh pair of phyllopods is sexually dimorphic between the sexes and does not bear a metepipodite (Fig. 3A, 4A, B, C, 5A, B). Each metepipodite is a flattened leaf-like oval structure (Fig. 3A, C, 5G), with average minimum and maximum dimensions of 225±50 µm and 486±84 µm. Metepipodites 1 and 2 are smaller (Fig. 3A).

Internally, we observed a longitudinal digestive tract, and a pair of maxillary glands located on each side of the digestive tract in the anterior part of the body (Fig. 6).

3.3. Histology and immunolocalization of Na^+/K^+-ATPase (NKA)

Metepipodites are flat structures formed of two identical facing monolayered epithelia covered by a thin cuticle, limiting a hemolymph lacuna (Fig. 5). A hemolymphatic space at the base of each metepipodite allows a communication with the phyllopod (Fig. 5C, D). NKA localization was visualized using immunohistochemical analysis of longitudinal and transverse sections. An intense immunostaining throughout most of the cells was observed in the epithelium of the ten pairs of metepipodites (Figs 3B, C, 4C, 5). The immunopositive cells were large (57±3 µm cellules) and contained a voluminous nucleus with average diameter of 10±1 µm (Fig. 5F, F'). Immunostaining intensity appears lower in some cells (Figs 3C, 5G).

The semi-quantification of fluorescence intensity of metepipodites showed no significant difference between the different metepipodites and among the analyzed salinities and an overall high variability was observed between animals (Fig. 2S).

A positive immunoreactivity for Na^+/K^+-ATPase was detected in the maxillary glands, where a strong immunostaining was observed in the epithelium of the efferent tubule and in the excretory canal (Fig. 6C-H). The proximal coelomic sac was not immunostained (Fig. 6C). The anterior digestive tract revealed a positive immunolabelling in the basal cell part as shown in Fig. 6D-F.

Negative control sections without the primary antibody did not show immunolabelling in any organ or tissue (not shown).

4. Discussion

Brine shrimps, *Artemia* species, are usually considered as extremophiles especially for their ability to face challenging salinities (up to 10-fold that of standard seawater) considered lethal for the majority of other aquatic species (Gajardo and Beardmore, 2012). Such environmental pressures demand an ability to regulate hemolymph osmolytes according to the external medium via powerful osmoregulatory mechanisms (Campbell et al., 2012; Charmantier et al., 2009; Freire et al., 2003). Blood osmolality change is often used as an indicator for osmoregulatory acclimation and tolerance to salinity stress (Varsamos et al., 2005). This study has confirmed the hypo-osmotic capacity of *Artemia* adults that can maintain their hemolymph osmolality up to 10 fold lower than their surrounding environment (for example hemolymph osmolality of 608 ±16 $mOsm.Kg^{-1}$ in a medium at 6192 $mOsm.Kg^{-}$

309 [1], 212 ppt). Due to these exceptional physiological abilities, brine shrimps are considered the
310 most powerful hypo-osmoregulators among aquatic metazoans, with the highest tolerance to
311 salinity (Cole and Brown, 1967). Extensive similar studies have concluded that the
312 hemolymph osmotic pressure was markedly hypotonic even in the most concentrated media
313 (Medwedewa, 1927; Plattner, 1955). Holliday *et al.* (1990) stated that *A. salina* is a weak
314 hyporegulator in 50 % SW and an increasingly strong hyporegulator in 100 %, 200 % and 400
315 % SW. Different studies have also shown a similarity between the mechanisms of
316 osmoregulation in *Artemia* adults and those proposed for marine teleosts and hypo-regulating
317 crustaceans (Croghan, 1958b, c, d; Copeland, 1967; Thuet *et al.*, 1968; Smith, 1969a, b).
318 Croghan (1958b, c, d), in an extensive study of osmoregulation in brine shrimps, has shown
319 that they have well-developed active mechanisms for absorbing NaCl from the gut lumen to
320 the hemolymph, resulting in a passive influx of water to hemolymph that compensates water
321 lost by osmosis to the external concentrated medium (Croghan, 1958d). Sodium and chloride,
322 which also enter the body through diffusion given their high concentration in the external
323 medium, are excreted to the medium by specialized organs.
324
325 Na^+/K^+-ATPase is known as the major driving force that ensures ion exchanges (Cieluch et
326 al., 2004; Geering, 2008; Lignot et al., 1999; Lignot and Charmantier, 2001; Lucu and Towle,
327 2003; Thabet et al., 2016; Thuet et al., 1988) as well as generating an electrical gradient
328 fuelling other transporters (Campbell et al., 2012; Esbaugh et al., 2019; Pivovarov et al.,
329 2019; Sáez et al., 2009). Its abundance in an organ suggests an involvement in ion transport.
330 The present study affords an overview of the different organs involved in osmoregulation in
331 *A. salina* adults. Immunofluorescence staining of Na^+/K^+-ATPase was used in order to
332 localize ionocytes in these organs.
333 Previous studies first addressed osmoregulation in embryos and during early post-
334 embryonic development. Several extensive studies have reported that active ion excretion
335 mediated by Na^+/K^+-ATPase is carried out by the naupliar salt gland (or dorsal / neck / nuchal
336 organ) that develops in late pre-naupliar embryonic stages; this organ becomes apparently
337 functional shortly before hatching. Later in development, thoracic epipodites take over ion
338 transport according to the stage of development (Conte, 1984; Conte et al., 1977, 1972;
339 Mitchell and Crews, 2002; Peterson et al., 1978; Russler and Mangos, 1978; Thuet, 1982).
340 Working in naupliar larvae, Sun *et al.* (1991) reported that Na^+/K^+-ATPase α and β subunits
341 were immunolocalized in the basal membranes of the salt gland cells. The mRNA expression

of α1 and α2 paralogs was quantified in the same organs (Conte, 2008; Escalante et al., 1995; Sun et al., 1991).

In the present study, an intense Na^+/K^+-ATPase immunostaining throughout most of the cells was observed in the epithelium of the ten pairs of metepipodites. Our results confirm those found in earlier works that attributed active outward transport of ions to metepipodites in adults (Copeland, 1967; Croghan, 1958c; Holliday et al., 1990). In a major study using electron microscopy, Copeland (1967) concluded that the metepipodites represent "a highly specialized tissue for the secretion of salt and a special cell type found in these structures (the 'dark cell'), rich in mitochondria, is thought to be responsible for this ion transport". The numerous immunostained cells that we observed in metepipodites therefore correspond to the "dark cells" as described by Copeland (1967). As we detected no difference in immunostaining intensity among metepipodites, this suggests a similar cellular Na^+/K^+-ATPase content among different metepipodites and an involvement of all metepipodites in active transport. Later experimental findings conducted on crude homogenates of metepipodites revealed a very high specific enzyme activity of Na^+/K^+-ATPase, which increased proportionally with the salinity of the external medium (Holliday et al., 1990). A slight but not significant increase in immunostaining intensity has been observed between 60 and 139 ppt and could indicate a slightly increased Na^+/K^+-ATPase content within the cells lining phyllopods at 139 ppt. Recently, a preliminary report of Drenth (2017) confirmed the presence of Na^+/K^+-ATPase in a metepipodite of *A. franciscana* and the salt extrusion occurs in a mitochondrial rich, membraneous cell layer in the metepipodites of the brine shrimp. The same investigator suggested that brine shrimp upregulate only the α2 form of Na^+/K^+-ATPase in response to increasing salinity, while the α1 form remains relatively unchanged.

A positive immunoreactivity for Na^+/K^+-ATPase was also detected in the anterior digestive tract and in the maxillary glands. In these paired glands, Na^+/K^+-ATPase immunostaining was observed in the epithelium of the efferent tubule and of the excretory canal, while the coelomic sac remained unstained. Our results confirmed that these organs are also involved in ion transport and probably for a part in osmoregulatory processes. In the same context, Tyson (1969) had shown that the efferent duct of the maxillary gland of *A. salina* presents ultrastructural features typical of transporting epithelia. Holliday *et al.* (1990) measured a high Na^+/K^+-ATPase activity in the digestive tract. Studying the physiology of the gut in *A. salina* and its implication in osmoregulation, Croghan (1958c) found that the concentration of both sodium and chloride ions in the gut fluids was always lower than that in the hemolymph, pointing to an active uptake of NaCl across the gut epithelium, which in turn controls water

balance and prevents dehydration in hypertonic media. Indeed, Drenth (2017) confirmed the basolateral localization of Na^+/K^+-ATPase in the gut of *A. franciscana* adults, where ions and water are taken in from the environment into the hemolymph (Russler and Mangos, 1978).

5. Conclusion

In this work, we have focused on the hypo-osmoregulatory capacity of adult *A.salina* and particularly on their main organs involved in active ion transport. We have confirmed that brine shrimps are powerful hypo-osmoregulators as they keep their hemolymph osmolality strongly lower than even the most concentrated media. Immunofluorescence and whole mounts staining of Na^+/K^+-ATPase have been used to illustrate the histological and cellular structure of metepipodites related to osmoregulation; despite their major function, their functional histology had surprisingly not been re-addressed since the major works of the 1960's. We have also confirmed the involvement in osmoregulation of the maxillary glands and of the anterior part of the digestive tract.

Acknowledgements

The authors would like to thank Sophie Hermet for her assistance in histology and the Montpellier Ressources Imaging (MRI-DBS UM) platform and notably Elodie Jublanc for her help in confocal microscopy**.**

List of References

Abatzopoulos, T.J., Kappas, I., Bossier, P., Sorgeloos, P., Beardmore, J.A., 2002. Genetic characterization of *Artemia tibetiana* (Crustacea: Anostraca). Biol. J. Linn. Soc. 75, 333–344. https://doi.org/10.1046/j.1095-8312.2002.00023.x

Boudour-Boucheker, N., Boulo, V., Charmantier-Daures, M., Grousset, E., Anger, K., Charmantier, G., Lorin-Nebel, C., 2014. Differential distribution of V-type H^+-ATPase and Na^+/K^+-ATPase in the branchial chamber of the palaemonid shrimp *Macrobrachium amazonicum*. Cell Tissue Res. 357, 195–206. https://doi.org/10.1007/s00441-014-1845-5

Boudour-Boucheker, N., Boulo, V., Lorin-Nebel, C., Elguero, C., Grousset, E., Anger, K., Charmantier-Daures, M., Charmantier, G., 2013. Adaptation to freshwater in the palaemonid shrimp *Macrobrachium amazonicum*: comparative ontogeny of osmoregulatory organs. Cell Tissue Res. 353, 87–98. https://doi.org/10.1007/s00441-013-1622-x

Brisset, P., Versichele, D., Bossuyt, E., De Ruyck, L., Sorgeloos, P., 1982. High density flow-through

412 culturing of brine shrimp *Artemia* on inert feeds-preliminary results with a modified culture
413 system. Aquac. Eng. 1, 115–119. https://doi.org/10.1016/0144-8609(82)90003-6
414 Browne, R.A., Bowen, S.T., 1991. Taxonomy and population genetics of *Artemia*, in: Browne, R.A.,
415 Sorgeloos, P., Trotman, C.N.A. (Eds.), Artemia Biology. CRC Press, Boca Raton, Florida,
416 U.S.A, pp. 221–235.
417 Campbell, J., Samuel, M., Faria, C., 2012. Evolution of osmoregulatory patterns and gill ion transport
418 mechanisms in the decapod Crustacea : a review. J Comp Physiol B 182, 997–1014.
419 https://doi.org/10.1007/s00360-012-0665-8
420 Charmantier, G., 1998. Ontogeny of osmoregulation in crustaceans: a review. Invertebr. Reprod. Dev.
421 33, 177–190. https://doi.org/10.1080/07924259.1998.9652630
422 Charmantier, G., Charmantier-Daures, M., Towle, D., 2009. Osmotic and ionic regulation in aquatic
423 arthropods, in: Evans, D.H. (Ed.), Osmotic and Ionic Regulation: Cells and Animals. CRC Press,
424 New York, pp. 165–208.
425 Cieluch, U., Anger, K., Aujoulat, F., Buchholz, F., Charmantier-Daures, M., Charmantier, G., 2004.
426 Ontogeny of osmoregulatory structures and functions in the green crab *Carcinus maenas*
427 (Crustacea, Decapoda). J. Exp. Biol. 207, 325–336. https://doi.org/10.1242/jeb.00759
428 Cieluch, U., Anger, K., Charmantier-Daures, M., Charmantier, G., 2007. Osmoregulation and
429 immunolocalization of Na^+/K^+-ATPase during the ontogeny of the mitten crab *Eriocheir sinensis*
430 (Decapoda, Grapsoidea). Mar. Ecol. Prog. Ser. 329, 169–178.
431 https://doi.org/10.3354/meps329169
432 Cieluch, U., Charmantier, G., Grousset, E., Charmantier-Daures, M., Anger, K., 2005.
433 Osmoregulation, immunolocalization of Na^+/K^+-ATPase, and ultrastructure of branchial epithelia
434 in the developing brown shrimp, *Crangon crangon* (Decapoda, Caridea). Physiol. Biochem.
435 Zool. 78, 1017–1025. https://doi.org/10.1086/432856
436 Clegg, J., Trotman, C.N.A., 2002. Physiological and biochemical aspects of *Artemia* ecology. Artemia
437 Basic Appl. Biol. 1, 129–170. https://doi.org/10.1007/978-94-017-0791-6_3
438 Cole, G.A., Brown, R.J., 1967. The chemistry of *Artemia* habitats. Ecology 48, 858–861.
439 https://doi.org/10.2307/1933745
440 Conte, F.P., 2008. Molecular domains in epithelial salt cell NaCl of crustacean salt gland (*Artemia*).
441 Int. Rev. Cell Mol. Biol. 268, 39–57. https://doi.org/10.1016/S1937-6448(08)00802-2
442 Conte, F.P., 1984. Structure and function of the crustacean larval salt gland, in: Bourne, G.H.,
443 Danielli, J.F., Jeon, K.W. (Eds.), International Review of Cytology. Academic Press, pp. 45–106.
444 https://doi.org/10.1016/S0074-7696(08)61314-5
445 Conte, F.P., Droukas, P.C., Ewing, R.D., 1977. Development of sodium regulation and de novo
446 synthesis of Na^+, K^+-activated ATPase in larval brine shrimp, *Artemia salina*. J. Exp. Zool. 202,
447 339–361. https://doi.org/10.1002/jez.1402020306
448 Conte, F.P., Hootman, S.R., Harris, P.J., 1972. Neck organ of *Artemia salina* nauplii. J. Comp.

449 Physiol. 80, 239–246. https://doi.org/10.1007/bf00694838
450 Copeland, D.E., 1967. A study of salt secreting cells in the brine shrimp (*Artemia salina*). Protoplasma
451 63, 363–384.
452 Cortas, N., Arnaout, M., Salon, J., Edelman, I.S., 1989. Isoforms of Na, K-ATPase in *Artemia salina*:
453 II. Tissue distribution and kinetic characterization. J. Membr. Biol. 108, 187–195.
454 https://doi.org/10.1007/bf01871029
455 Croghan, P.C., 1958a. The survival of *Artemia salina* (L.) in various media. J. Exp. Biol. 35, 213–218.
456 Croghan, P.C., 1958b. The osmotic and ionic regulation of *Artemia salina* (L.). J. Exp. Biol. 35, 219–
457 233.
458 Croghan, P.C., 1958c. The mechanism of osmotic regulation in *Artemia salina* (L.): the physiology of
459 the branchiae. J. Exp. Biol. 35, 234–242.
460 Croghan, P.C., 1958d. The mechanism of osmotic regulation in *Artemia salina* (L.): The physiology of
461 the gut. J. Exp. Biol. 35, 243–249.
462 Drenth, J., 2017. Altered Na, K-ATPase isoform expression in *Artemia franciscana* in response to
463 hypersaline environments. Thesis Diss. https://doi.org/10.30707/ETD2017.Drenth.J
464 Eads, B.D., 2004. Salty survivors: *Artemia*: basic and applied biology. J. Exp. Biol. 207, 1757–1758.
465 https://doi.org/10.1242/jeb.01005
466 Esbaugh, A.J., Brix, K. V, Grosell, M., 2019. Na^+, K^+-ATPase isoform switching in zebrafish during
467 transition to dilute freshwater habitats. Proc. R. Soc. B 286.
468 https://doi.org/10.1098/rspb.2019.0630
469 Escalante, R., García-Sáez, A., Sastre, L., 1995. In situ hybridization analyses of Na, K-ATPase alpha-
470 subunit expression during early larval development of *Artemia franciscana*. J. Histochem.
471 Cytochem. 43, 391–399. https://doi.org/10.1177/43.4.7897181
472 Freire, C.A., Cavassin, F., Rodrigues, E.N., Torres, A.H., McNamara, J.C., 2003. Adaptive patterns of
473 osmotic and ionic regulation, and the invasion of fresh water by the palaemonid shrimps. Comp.
474 Biochem. Physiol. Part A Mol. Integr. Physiol. 136, 771–778.
475 https://doi.org/10.1016/j.cbpb.2003.08.007
476 Gajardo, G.M., Beardmore, J.A., 2012. The brine shrimp *Artemia*: adapted to critical life conditions.
477 Front. Physiol. 3, 1–8. https://doi.org/10.3389/fphys.2012.00185
478 Gauthier, H., 1928. Recherches sur la faune des eaux continentales de l'Algérie et de la Tunisie.
479 Thesis Diss. Minerva, Alger, Algerie.
480 Geering, K., 2008. Functional roles of Na,K-ATPase subunits. Curr. Opin. Nephrol. Hypertens. 17,
481 526–532. https://doi.org/10.1097/MNH.0b013e3283036cbf
482 Gerber, L., Lee, C.E., Grousset, E., Blondeau-Bidet, E., Boucheker, N.B., Lorin-Nebel, C.,
483 Charmantier-Daures, M., Charmantier, G., 2016. The legs have it: In situ expression of ion
484 transporters V-type H^+-ATPase and Na^+/K^+-ATPase in the osmoregulatory leg organs of the
485 invading copepod *Eurytemora affinis*. Physiol. Biochem. Zool. 89, 233–250.

https://doi.org/10.1086/686323

Holliday, C.W., Roye, D.B., Roer, R.D., 1990. Salinity-induced changes in branchial Na^+/K^+-ATPase activity and transepithelial potential difference in the brine shrimp *Artemia sauna*. J. Exp. Biol. 151, 279–296.

Issartel, J., Boulo, V., Wallon, S., Geffard, O., Charmantier, G., 2010. Cellular and molecular osmoregulatory responses to cadmium exposure in *Gammarus fossarum* (Crustacea, Amphipoda). Chemosphere 81, 701–710. https://doi.org/10.1016/j.chemosphere.2010.07.063

Lavens, P., Sorgeloos, P., 1996. Manual on the production and use of live food for aquaculture., FAO Tech. Pap. Food and Agriculture Organization (FAO), Rome, Italy.

Lignot, J.-H., Charmantier-Daures, M., Charmantier, G., 1999. Immunolocalization of Na^+/K^+-ATPase in the organs of the branchial cavity of the european lobster *Homarus gammarus* (Crustacea, Decapoda). Cell Tissue Res. 296, 417–426. https://doi.org/10.1007/s004410051301

Lignot, J.-H., Charmantier, G., 2001. Immunolocalization of Na^+, K^+-ATPase in the branchial cavity during the early development of the european lobster *Homarus gammarus* (Crustacea, Decapoda). J. Histochem. Cytochem. 49, 1013–1023. https://doi.org/10.1177/002215540104900809

Lignot, J.-H., Susanto, G.N., Charmantier-Daures, M., Charmantier, G., 2004. Immunolocalization of Na^+, K^+-ATPase in the branchial cavity during the early development of the crayfish *Astacus leptodactylus* (Crustacea, Decapoda). Cell Tissue Res. 319, 331–339. https://doi.org/10.1007/s00441-004-1015-2

Lucu, Č., Towle, D.W., 2003. Na^+, K^+-ATPase in gills of aquatic crustacea. Comp. Biochem. Physiol. Part A Mol. Integr. Physiol. 135, 195–214. https://doi.org/10.1016/S1095-6433(03)00064-3

Medwedewa, N.B., 1927. Über den osmotischen Druck der Hämolymphe von *Artemia salina*. J. Comp. Physiol. A Neuroethol. Sensory, Neural, Behav. Physiol. 5, 547–554.

Mitchell, B., Crews, S.T., 2002. Expression of the *Artemia* trachealess gene in the salt gland and epipod. Evol. Dev. 4, 344–353. https://doi.org/10.1046/j.1525-142X.2002.02023.x

Morohashi, M., Kawamura, M., 1984. Solubilization and purification of *Artemia salina* (Na, K)-activated ATPase and NH_2-terminal amino acid sequence of its larger subunit. J. Biol. Chem. 259, 14928–14934.

Ouattara, N., Bodinier, C., Nègre-Sadargues, G., D'Cotta, H., Messad, S., Charmantier, G., Panfili, J., Baroiller, J.-F., 2009. Changes in gill ionocyte morphology and function following transfer from fresh to hypersaline waters in the tilapia *Sarotherodon melanotheron*. Aquaculture 290, 155–164. https://doi.org/10.1016/j.aquaculture.2009.01.025

Peterson, G.L., Ewing, R.D., Conte, F.P., 1978. Membrane differentiation and de novo synthesis of the (Na^+/ K^+)-activated adenosine triphosphatase during development of *Artemia salina* nauplii. Dev. Biol. 67, 90–98. https://doi.org/10.1016/0012-1606(78)90302-0

Pivovarov, A.S., Calahorro, F., Walker, R.J., 2019. Na^+ / K^+ - pump and neurotransmitter membrane

receptors. Invertebr. Neurosci. 19, 1–16. https://doi.org/10.1007/s10158-018-0221-7

Plattner, F., 1955. Der osmotische Druck von *Artemia salina*. Pflüger's Arch. für die gesamte Physiol. des Menschen und der Tiere 261, 172–182. https://doi.org/10.1007/bf00369788

Post, F.J., Youssef, N.N., 1977. A procaryotic intracellular symbiont of the Great Salt Lake brine shrimp *Artemia salina* (L.). Can. J. Microbiol. 23, 1232–1236. https://doi.org/10.1139/m77-184

Riou, V., Ndiaye, A., Budzinski, H., Dugué, R., Le Ménach, K., Combes, Y., Bossus, M., Durand, J.-D., Charmantier, G., Lorin-Nebel, C., 2012. Impact of environmental DDT concentrations on gill adaptation to increased salinity in the tilapia *Sarotherodon melanotheron*. Comp. Biochem. Physiol. Part C Toxicol. Pharmacol. 156, 7–16. https://doi.org/10.1016/j.cbpc.2012.03.002

Russler, D., Mangos, J., 1978. Micropuncture studies of the osmoregulation in the nauplius of *Artemia salina*. Am. J. Physiol. Integr. Comp. Physiol. 234, R216–R222. https://doi.org/10.1152/ajpregu.1978.234.5.R216

Sáez, A.G., Lozano, E., Zaldívar-Riverón, A., 2009. Evolutionary history of Na, K-ATPases and their osmoregulatory role. Genetica 136, 479–490. https://doi.org/10.1007/s10709-009-9356-0

Smith, P.G., 1969a. The ionic relations of *Artemia salina* (L.): I. Measurements of electrical potential difference and resistance. J. Exp. Biol. 51, 727–738.

Smith, P.G., 1969b. The ionic relations of *Artemia salina* (L.): II. Fluxes of sodium, chloride and water. J. Exp. Biol. 51, 739–757.

Sorgeloos, P., Lavens, P., Léger, P., Tackaert, W., Versichele, D., 1986. Manual for the culture and use of brine shrimp *Artemia* in aquaculture. Artemia Ref. Center, Faculty of Agriculture, State Univ. Ghent, Belgium.

Sucré, E., Vidussi, F., Mostajir, B., Charmantier, G., Lorin-Nebel, C., 2012. Impact of ultraviolet-B radiation on planktonic fish larvae: Alteration of the osmoregulatory function. Aquat. Toxicol. 109, 194–201. https://doi.org/10.1016/j.aquatox.2011.09.020

Sun, D.Y., Guo, J.Z., Hartmann, H.A., Uno, H., Hokin, L.E., 1992. Differential expression of the alpha 2 and beta messenger RNAs of Na, K-ATPase in developing brine shrimp as measured by in situ hybridization. J. Histochem. Cytochem. 40, 555–562. https://doi.org/10.1177/40.4.1313064

Sun, D.Y., Guo, J.Z., Hartmann, H.A., Uno, H., Hokin, L.E., 1991. Na, K-ATPase expression in the developing brine shrimp *Artemia*. Immunochemical localization of the alpha-and beta-subunits. J. Histochem. Cytochem. 39, 1455–1460. https://doi.org/10.1177/39.11.1655875

Tagorti, M.A., Essefi, E., Touir, J., Guellala, R., Yaich, C., 2013. Geochemical controls of groundwaters upwelling in saline environments : Case study the discharge playa of Sidi El Hani (Sahel, Tunisia). J. African Earth Sci. 86, 1–9. https://doi.org/10.1016/j.jafrearsci.2013.05.004

Thabet, R., Rouault, J., Ayadi, H., Leignel, V., 2016. Structural analysis of the α subunit of Na^+/K^+ ATPase genes in invertebrates. Comp. Biochem. Physiol. Part B Biochem. Mol. Biol. 196, 11–18. https://doi.org/10.1016/j.cbpb.2016.01.007

Thuet, P., 1982. Adaptations écophysiologiques d'*Artemia* (Crustacé, Branchiopode, Anostracé) aux variations de salinité. Bull. la société d'écophysiologie 7, 203–225.

Thuet, P., Charmantier-Daures, M., Charmantier, G., 1988. Relation entre osmorégulation et activités d'ATPase Na^+-K^+ et d'anhydrase carbonique chez larves et postlarves de *Homarus gammarus* (L.)(Crustacea: Decapoda). J. Exp. Mar. Bio. Ecol. 115, 249–261.

Thuet, P., Motais, R., Maetz, J., 1968. Les mécanismes de l'euryhalinité chez le crustacé des salines *Artemia salina* L. Comp. Biochem. Physiol. 26, 793–818.

Tyson, G.E., 1969. Intercoil connections of the kidney of the brine shrimp, *Artemia salina*. Z. Zellforsch. 100, 54–59.

Varsamos, S., Nebel, C., Charmantier, G., 2005. Ontogeny of osmoregulation in postembryonic fish: a review. Comp. Biochem. Physiol. Part A Mol. Integr. Physiol. 141, 401–429.

Ziegler, A., 1997. Immunocytochemical localization of Na^+, K^+-ATPase in the calcium-transporting sternal epithelium of the terrestrial isopod *Porcellio scaber* L . (Crustacea). J. Histochem. Cytochem. 45, 437–446. https://doi.org/10.1177/002215549704500311

Legends of Figures

Abbreviations. ADT: anterior digestive tract; Cs: coelomic sac; E: eye; EC: excretory canal; Me: metepipodite; MG: maxillary gland; N: nucleus; Ph: phyllopod; PI: posterior intestine; T: tubule.

Fig. 1. Geographical location of the Sebkha of Sidi El Hani (Tunisia). Google Earth Pro V. 7.3.2.5776.

Fig. 2. Adult *Artemia salina*. Osmotic pressure of the hemolymph of animals maintained at three different salinities (60 ppt: 1737 $mOsm.Kg^{-1}$, 139 ppt: 4064 $mOsm.Kg^{-1}$, 212 ppt: 6192 $mOsm.Kg^{-1}$, N=8-12). The dotted line is the isosmotic line. Different letters indicate significant differences ($p<0.001$).

Fig. 3. Adult *Artemia salina*. Morphology and localization of metepipodites (Me) and maxillary glands (MG). (A) Dorsal view showing the eleven pairs of phyllopods (Ph) and the ten pairs of metepipodites. (B), (C) Whole-mounts and immunolocalization of Na^+/K^+-ATPase; (B) Anterior view with immunostaining in the two maxillary glands and in one metepipodite 1; (C) Median view with several phyllopods and immunostained metepipodites. Scale bars: (A) 500 µm; (B), (C) 200 µm.

Fig. 4. Adult *Artemia salina.* Localization of metepipodites (Me) on phyllopods (Ph). (A), (B) Longitudinal vertical and horizontal histological sections. (C) Longitudinal horizontal section:

immunolocalization of Na^+/K^+-ATPase in metepipodites 1-9 attached to phyllopods. Scale bars: (A), (B) 500 µm, (C) 40 µm.

Fig. 5. Adult *Artemia salina.* Histological structure and immunolocalization of Na^+/K^+-ATPase (NKA) and DNA staining of nuclei on phyllopods and metepipodites sections. (A), (B), (F), (F') Merged staining of Na^+/K^+-ATPase (green) and DNA (blue). (C), (D), (E) Phyllopds bearing metepipodites with NKA immunostaining (D, E) or Trichrome Masson's staining (C). (G) Immunolocalization of NKA on metepipodites in horizontal (Me4) and transverse (Me5, 6) sections. Scale bars: (A), (B) 40 µm; (C), (D), (E), (F), (G) 20 µm; (F') 5 µm.

Fig. 6. Adult *Artemia salina.* Histological structure, whole-mounts and immunolocalization of Na^+/K^+-ATPase (NKA) in the anterior digestive tract (ADT), in the maxillary gland (MG), and in metepipodite (Me). (A), (B) Transverse histological sections of the anterior digestive tract and of the maxillary gland. (C), (D), (E) NKA localization in transverse sections of the anterior digestive tract and of the maxillary gland. (F) Horizontal section of the anterior digestive tract and of the two maxillary glands. (G), (H) Whole mounts showing NKA localization in the maxillary gland and metepipodite 1. Scale bars: (A), (B), (C), (D), (F) 20 µm; (E) 40 µm; (G) 200 µm; (H) 50 µm.

Fig. 1S. Present results (in red) and previous knowledge on osmoregulation in the branchiopod *Artemia* at different development stages involving different osmoregulatory organs.

Fig. 2S. Adult *Artemia salina*. Relative immunostaining intensity for Na^+ /K^+-ATPase (NKA) in the different metepipodites (1-10) and its difference according to different salinities. (A) Comparison between the metepipodites (1-10) regardless of salinity (N=5-6). (B) Comparison between the studied salinities regardless of the location of metepipodite (N=3-12).

Fig. 1.

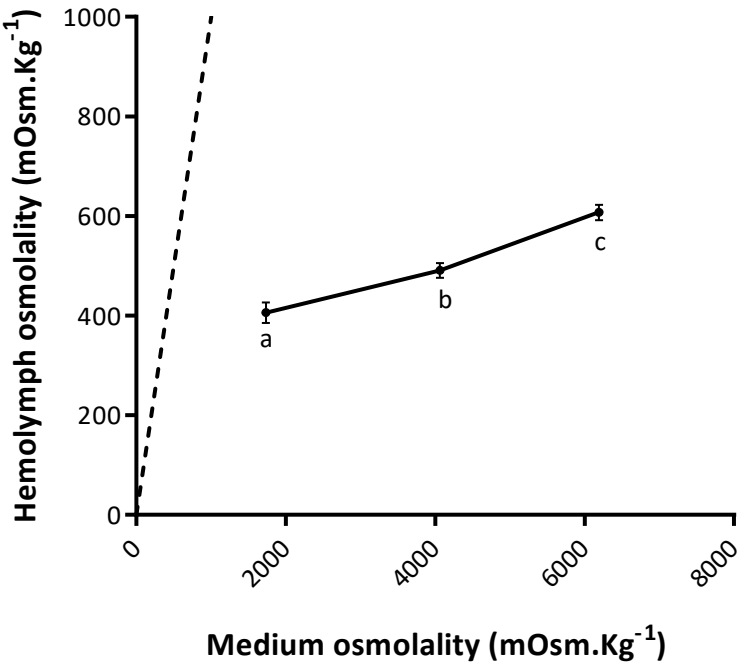
Hemolymph osmolality (mOsm.Kg-1)
1000
800
600
400
200
0
0
2000
4000
6000
8000
a
b
c
Medium osmolality (mOsm.Kg-1)

Fig. 2.

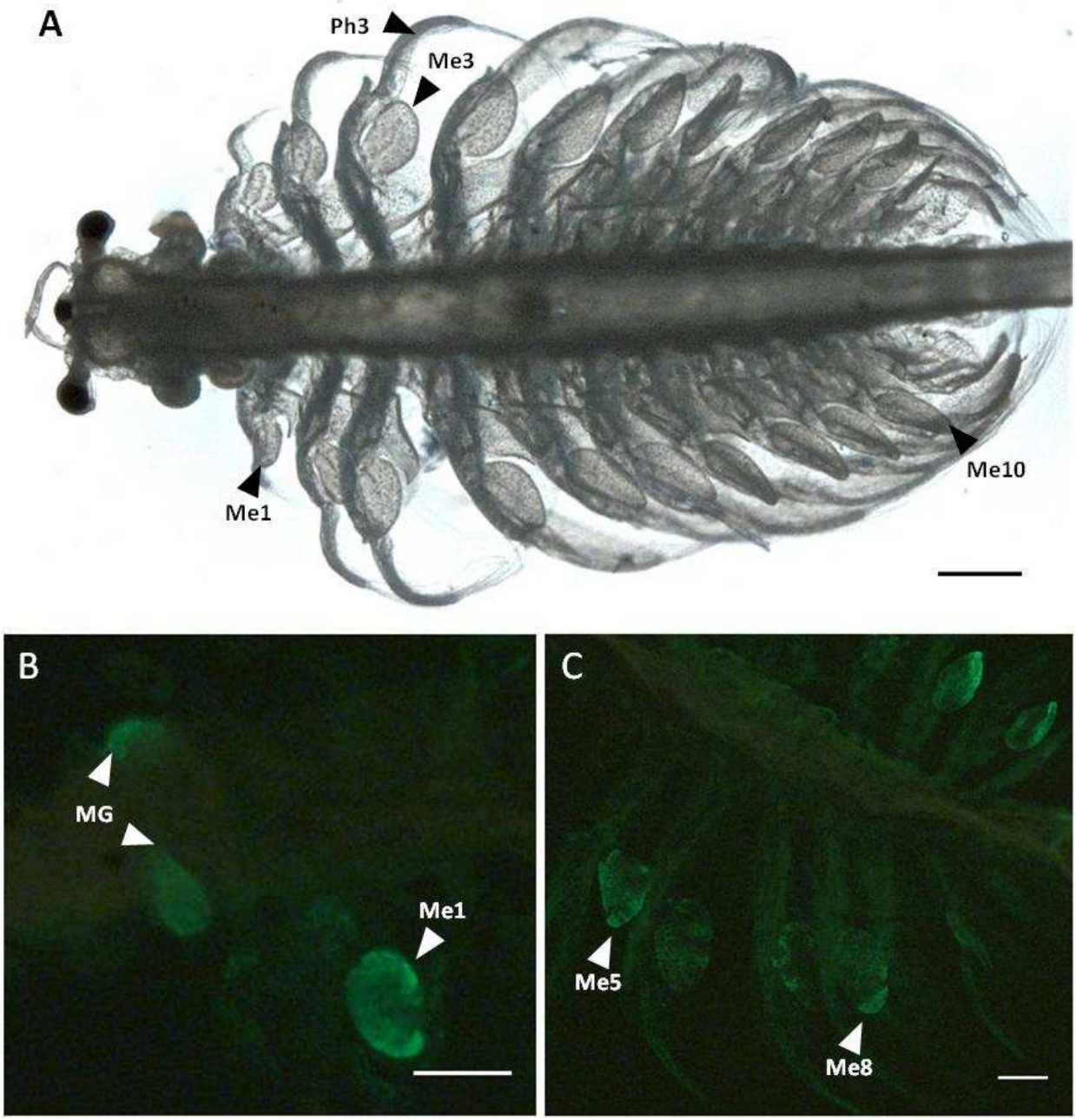

660
661 **Fig. 3.**

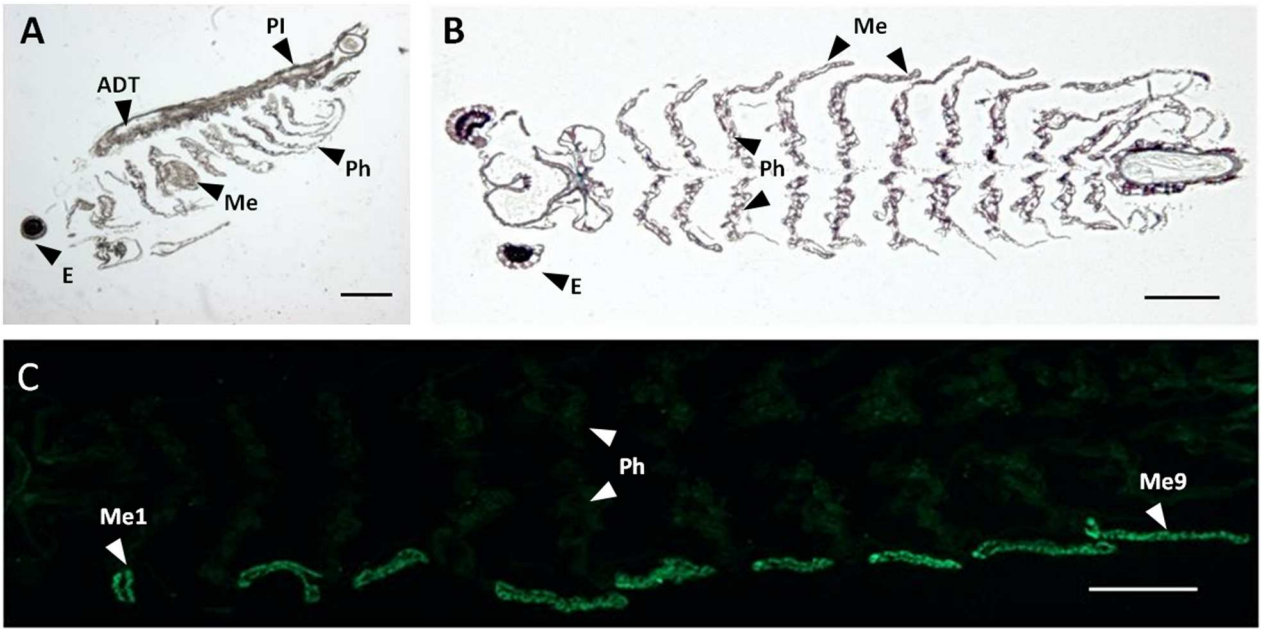

662
663 **Fig. 4.**
664

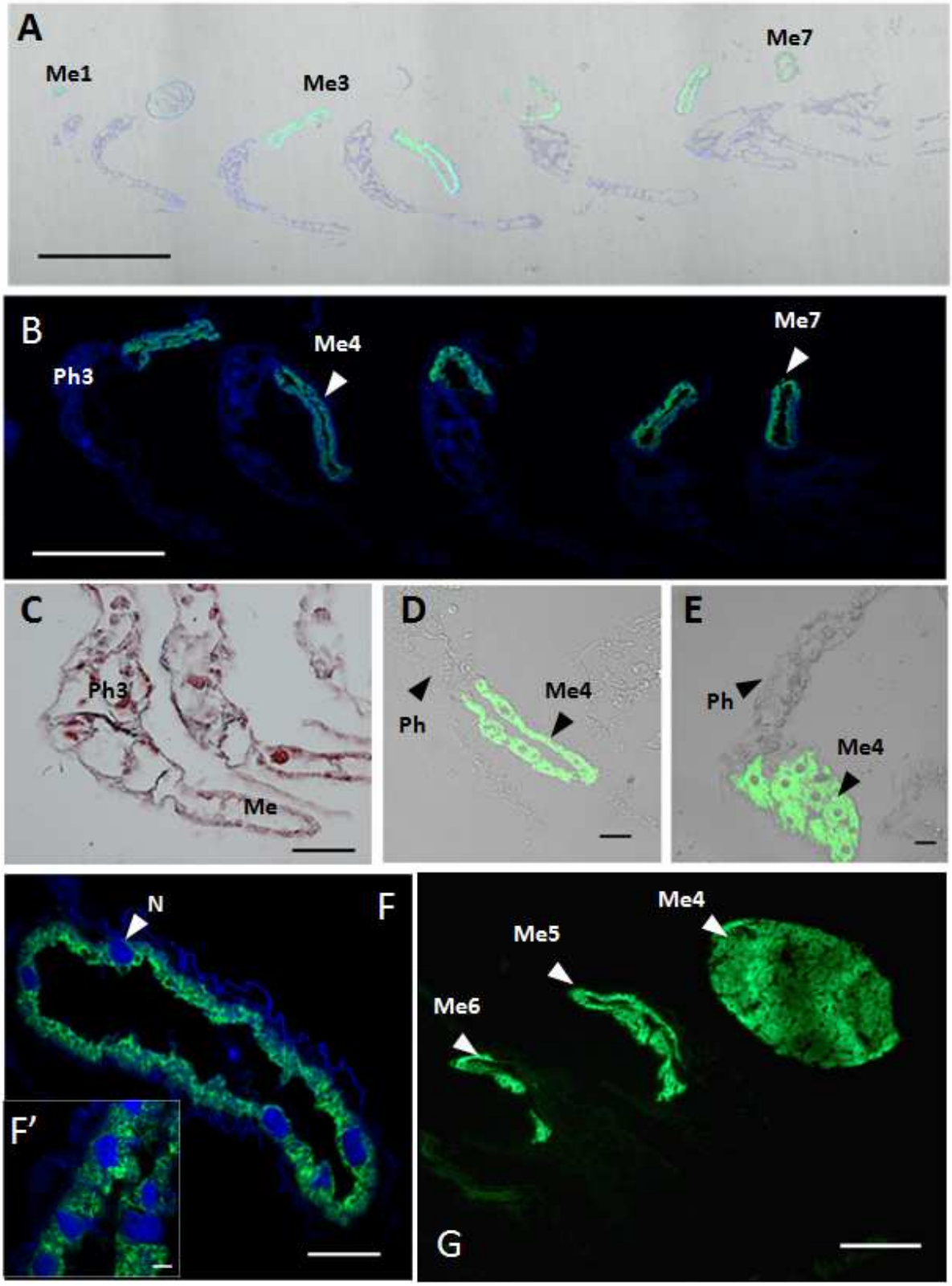

665
666 **Fig. 5.**
667

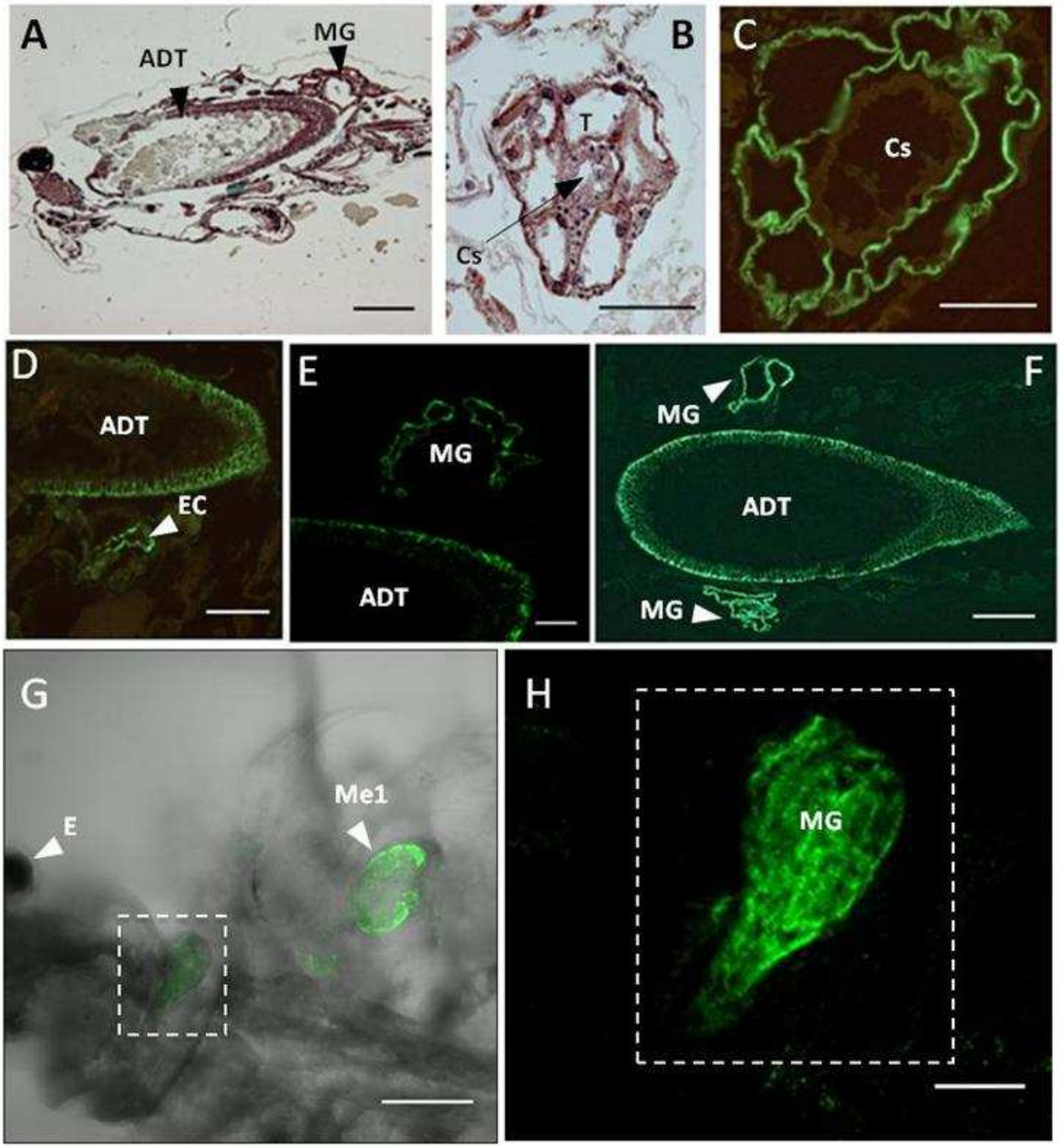

668
669 **Fig. 6.**
670
671

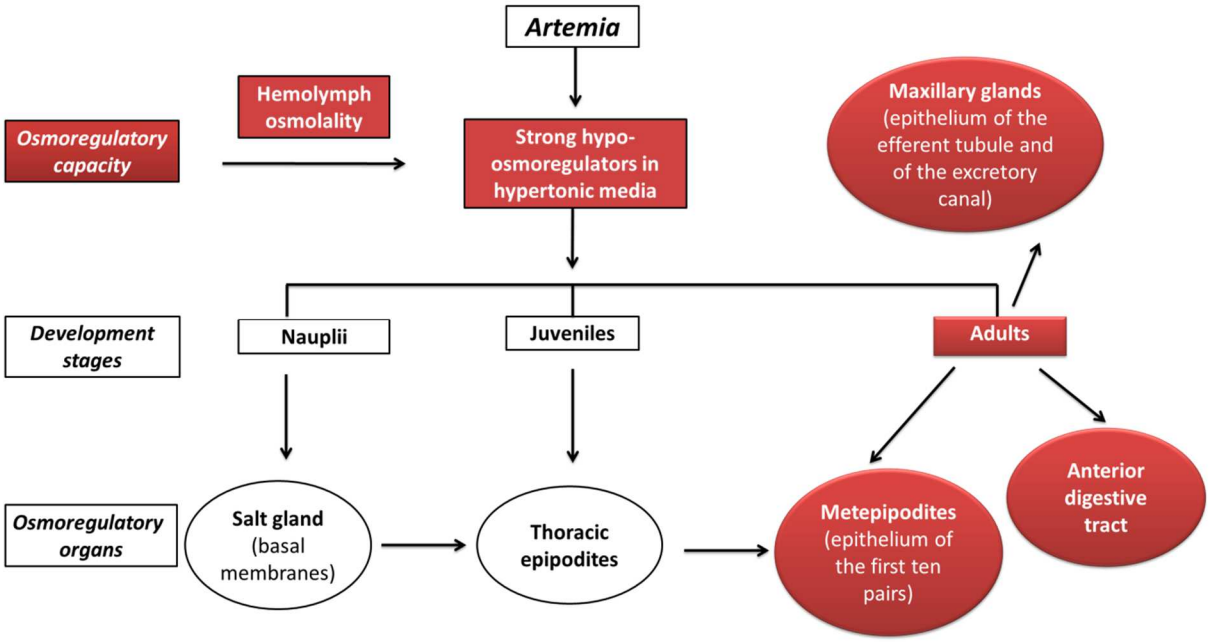

672
673
674
675
676 **Fig. 1S.**
677

678
679

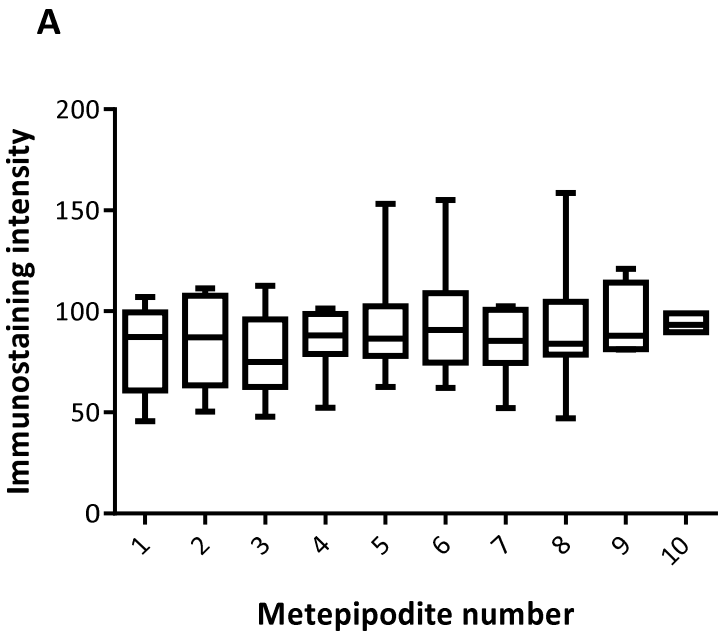

680
681

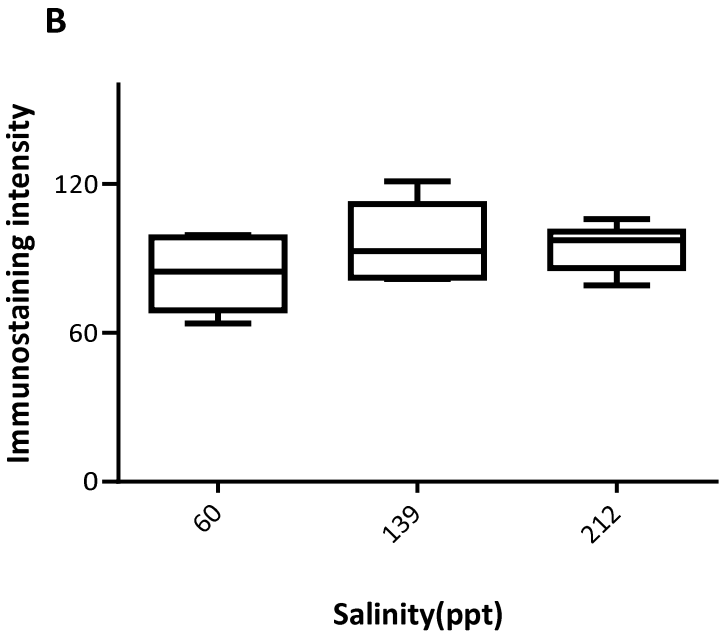

682
683 **Fig. 2S.**
684
685
686